Analysis and Confirmation of the "Superwave-as-Transitory–OOP-Peak" Hypothesis

Mitchell R. Swartz[1] and Lawrence P.G. Forsley[2]
[1] *JET Energy, Inc. Wellesley, MA 02481 (USA)*
[2] *JWK Technologies Corporation, Annandale, Virginia*

Abstract - The optimal operating point (OOP) approach to LANR has successfully enabled the construction of more robust and reproducible LANR devices. This paper considers the "Superwave-as-a-Transitory OOP" hypothesis as a possible explanation of the "superwave" results. Deconvolution of the input power of the "superwave" function shows that LANR activity results arise from inadvertently driving a LANR sample through its OOP, at least during part of the duty cycle, thereby giving rise to the desired reaction(s).

Index Terms - Optimal operating point, palladium, superwave, hyperdrive, Input Power Space, Equivalent Electrical Input Power Transform, LANR

1.1 Introduction

There has been discussion of, and interest in, the potential of the "superwave", an Israeli-designed nonlinear function (1) used to drive lattice assisted nuclear reactions (LANR). Reports (2) include power gains of 3.9 using a LANR glow discharge experiment, and HAD lasting ~10 hours resulting in an energy gain of 6.7 times the input energy. They then reported (3) excess heat with seven different Pd foils provided by Dr. Vittorio Violante of ENEA Frascatti. The maximum power gain was 6.0. The longest run was 134 hours (power gain 1.5). There have been many theories proposed for the purported success of the superwave with respect to reported elicited excess heat (1), although full details of its achieved peak output powers, excess power gains, etc. have not been published. But, its waveform, and some elements of its construction have been reported sufficiently to enable others to hypothesize theoretical reasons predicated upon the superwave function's extreme nonlinearity. This report adds another, best understood by converting LANR-driving time functions to their equivalent Input Power Space (Figure 1), as is done with OOP manifolds.

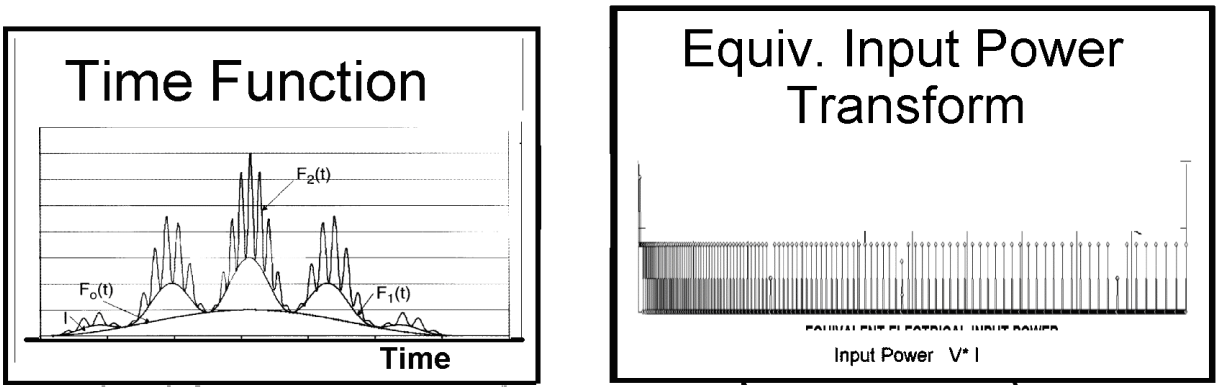

Figure 1. Superwave (after Dardik) and its Equivalent Input Power Transform (after Swartz)

1.2 Background: Optimal Operating Points (OOP)

Over the years, the optimal operating point approach to LANR has been quite successful (4-9). Figure 2 shows an OOP manifold for the excess power output (watts) for a heavy water deuterium-loaded Phusor®-type LANR cathode and an ohmic joule control, for 1 to 7 watts input electrical power. For this type LANR device, the optimal operating point (OOP) is located at ~3.6 watts input power. Figure 2 also shows the excess power output observed for several ohmic joule (thermal) controls ("CONTROLS") which, as can be seen, demonstrated "under-unity" performance and failed to demonstrate excess power gain at several different input electrical powers. This confirms and validates the data by providing a control.

For the LANR behavior (confer Figure 2), two regions of less than peak optimal output can be seen, which occur because of inadequate loading (to the left of the peak) and wasteful electrolysis (to the right of the peak). Driving with electrical input power beyond the peak optimal operating point (OOP) does not improve the production of the desired product, but instead yields a falloff of the production rates despite increasing input power.

This OOP operation is important because for a LANR system exhibiting excess power gain and excess heat, or helium-4 or tritium production, under application of input electrical power, the optimal operating point (OOP) is the input electrical power at which there is a relatively narrow peak along the input power axis. This OOP, the peak point to drive the system is, however, but one focus at which the system can be driven. The other possible points at which the system can be driven, are in the "optimal operating point manifold", a virtual curve surrounding the ensemble of data points, but not at the peak. In retrospect, many negative LANR reports appear to have occurred due to a failure to operate the LANR system at, or near, the optimal operating point.

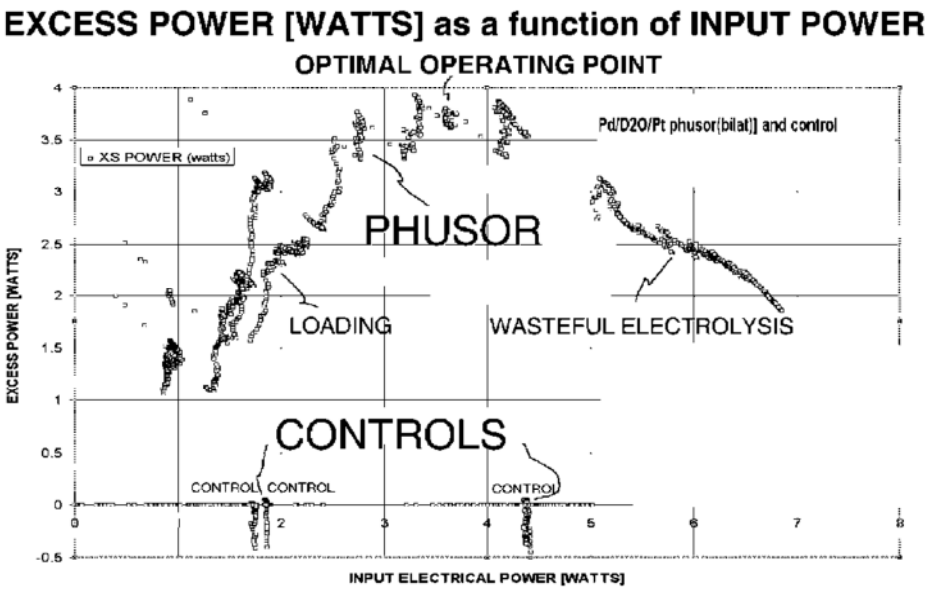

Figure 2. OOP Manifold of a Pd/D_2O/Pt Phusor®-type system - excess power [watts].

The OOP manifolds reflect the relatively narrow peak of the biphasic production curves (for excess power, helium-4 or tritium production) as a function of input electrical power. The height of the data points, which together comprise the OOP manifold, is a measure of the product output or excess power gain of that LANR specimen, material, or device, at that particular input drive point along the input electrical power axis. Figure 3 shows some OOP Manifolds from independent LANR investigators as a function of input electrical power [log watts]. The groups of data, such as excess heat in palladium in heavy water, incremental helium-4 production from palladium loaded in heavy water, and incremental tritium generated from codeposition and from palladium in heavy water, are connected with lines, comprising optimal operating point manifolds. The vertical axis represents the observed outputs, and is linear. Curves (manifolds) connect the data points of each group.

In this system approach, the relative height of each curve along the input electrical power axis heralds the product output from a LANR system (Figures 2 and 3). Thus, this approach to examining LANR output data differs from other ways. In this approach, there appears a maximum of the biphasic product-output rate curve for excess heat, excess power gain (as in Figure 2), or de novo incremental helium-4 or tritium production (as in Figure 3) when presented as a function of the input electrical power.

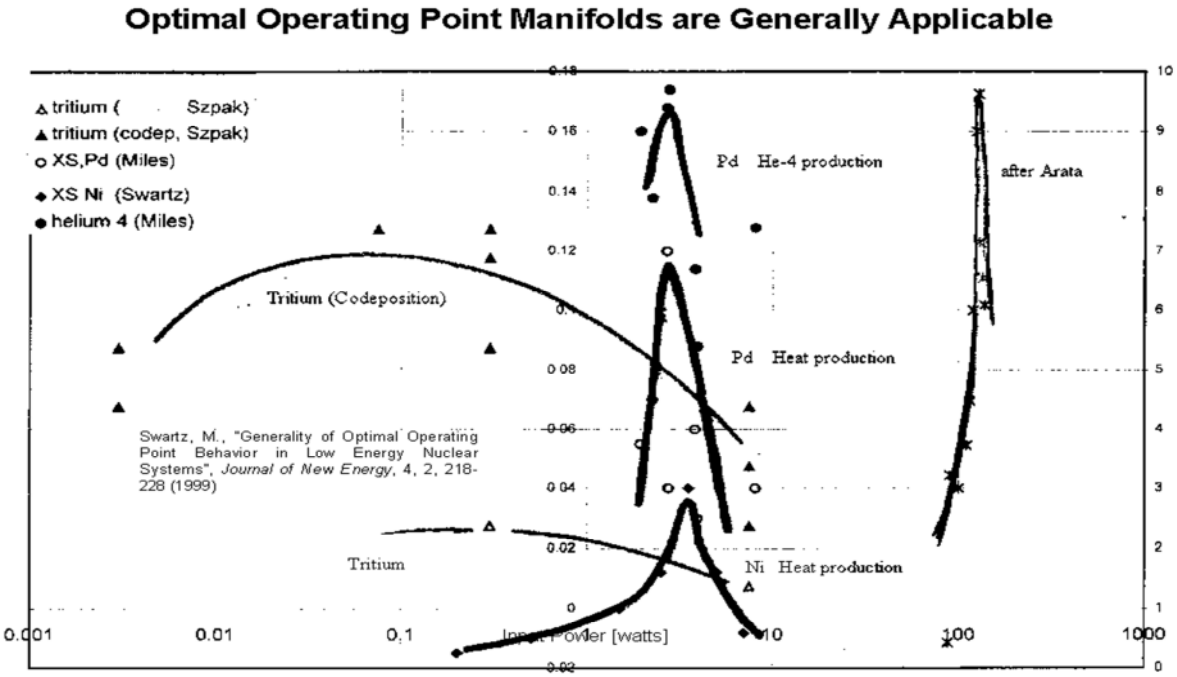

Figure 3. OOP Manifolds shown by log input electrical power [watts].

Several things should immediately pop out as we look at the OOP manifold curves (Figure 3) First, OOP manifolds appear to be universal. They describe a large group of LANR systems. These include power gain in high impedance [Pd/D_2O/Pt, Pd/D_2O/Au] and in Ni/$H_2O_xD_2O_{1-x}$/Pt and Ni/$H_2O_xD_2O_{1-x}$/Au] Phusor®-type LANR devices, and in codeposition systems and codeposition LANR devices, heavy water helium production and excess heat production from Pd/D2O systems; tritium generated from codeposition and Pd/D_2O systems; power gain in light water and mixed light/heavy water nickel LANR devices; and excess heat and helium production in palladium-black systems (4-9).

Second, LANR production data, organized along the electrical input power axis, dispels the purported LANR “irreproducibility” debate. Note that OOP manifolds appear as one arranges enough product-formation data points over a wide enough input power range. In the case of Figure 3, the OOP manifolds of many credible investigators using disparate LANR systems show that their experimental work product can be clearly organized along the electrical input power axis. Suddenly, the "irreproducibility" disappears, and what was disordered becomes ordered. Third, LANR is better controlled and understood by the recognition, and use, of Optimal Operating Point (OOP) manifolds.

2.1 Hypothesis Tested

The optimal operating point (OOP) approach to LANR has been successful and has enabled the construction of robust and more reproducible LANR devices. In that light, this paper considers the “Superwave-as-a-Transitory OOP” hypothesis as a possible explanation of the

"superwave" results. Lawrence Forsley first proposed that the reported success of the application of the superwave to LANR samples might have its success secondary to the fact that the superwave is, on occasion, driving the LANR samples through their optimal operating point (OOP). To test that hypothesis, a mathematical analysis designed to transform temporal waveforms to V*I Space was used to test its validity. By this investigational method we have deconvolved functions, transforming the time functions (the left hand side of Figure 1) to EIP Space (right side of Figure 1), including the "superwave"-type function. This preliminary analysis shows that it is possible that the LANR activity results of the superwave arises from inadvertently driving a LANR sample through its optimal operating point, at least during part of the duty cycle, thereby giving rise to the desired reaction(s). The histograms support the Hypothesis, offering a possible explanation of the reported results.

2.2 Experimental

As part of ongoing efforts, theoretical algorithms in Liberty Basic were used to analyze and transform various non-linear time functions representing electrical input current, potential, or power to an input power "space" dependent upon input power. For this first order model, the LANR system was modeled as a simple resistor, without capacitive or inductive effects even though LANR systems are far more complicated than a lumped parameter electrical device. When input electrical current was considered, the input electrical power was assumed to be, $P_{in} = R*I(t)*I(t)$. The program analyzed each waveform's cycle from 0 to 2π radians by sampling through incremental small, differential angles of the waveform, each one thousandth of the interval. The input power was derived, and generated a histogram of the number of time intervals had each electrical input energy, between P_i and $P_i + \Delta P$, from 0 to the maximum. The output deconvolution of equivalent electrical input power (EIP) was thus determined.

3.1 Results - Unmodulated Sinusoidal Function

The histograms of the generated equivalent electrical input powers are shown in Figure 4. The x-axis represents equivalent electrical input power. It goes from zero to the full $R*(I_0)^2$ watts. The height of the histogram at each point shows the relative proportion of input power between P_i and $P_i + \Delta P$ for each interval. Within Figure 4, the histograms for the simplest functions, $\sin(\omega*t)$ and $\sin(\omega*t)*\sin(7\omega*t)$, can be seen. The upper curve is the simplest sine wave, $\sin(\omega*t)$, which has a roughly equal distribution of its "energy" into all increment equivalent input power bins, over the interval of 0 to $P= R*(I_0)^2$ watts. Grouping input powers into low-, mid- and high-power regions shows that for the simple sinusoidal function there is good distribution over the three regions (37, 24, and 39, respectively). [The bin with the highest density on the histogram analysis was bin 999 with n=22.]

3.2 Single modulated Sinusoidal Function

The lower function shown in Figure 4 is the result of equivalent electrical input power (EIP) for the binary function $\sin(\omega*t)*\sin(7\ \omega*t)$, a 'second order' or 'single modulated' sinusoidal function. Its EIP histogram should be compared to the simplest function, $\sin(\omega*t)$, above it. The distribution of equivalent electrical input power (EIP) of the modulated sinusoidal function is

not similarly uniform over the interval of 0 to P= $R*(I_0)^2$ watts. Grouping input powers into low-, mid-, and high power regions yielded 64, 23, and 13, respectively. The single modulation yields inhomogeneity and a shift toward lower equivalent input powers. [The bin with the highest density on the histogram analysis was bin 20 with n=20.] In this case, note that the EIP histogram changes significantly by the single modulation.

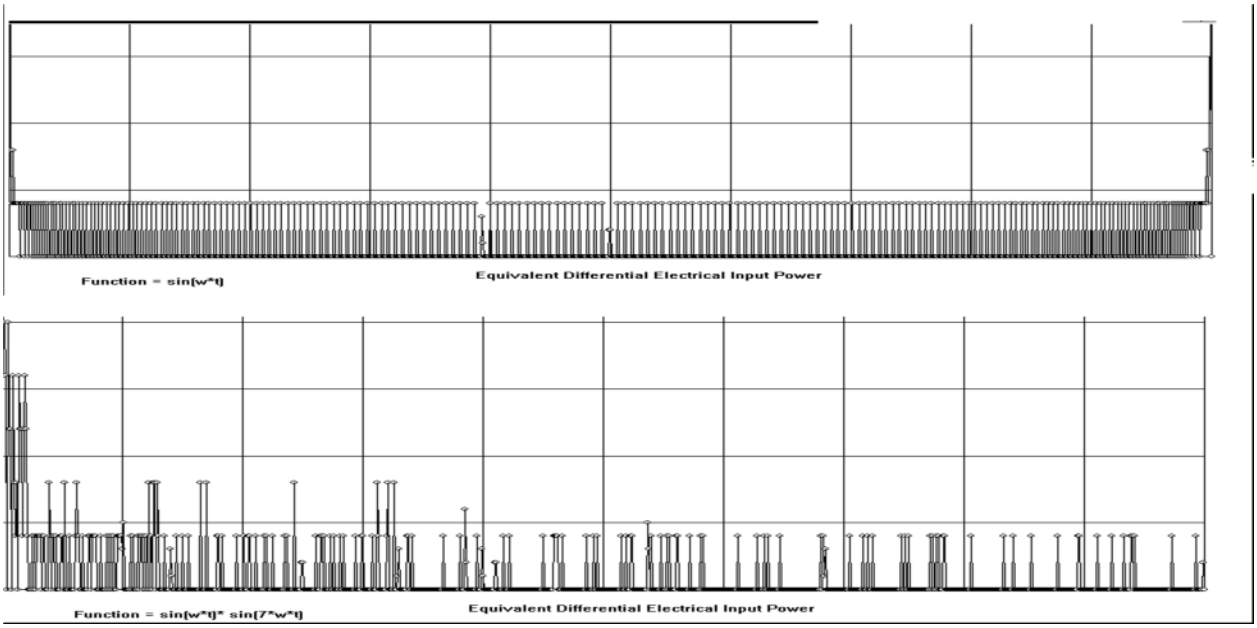

Figure 4. EIP Histograms of 1st, 2nd Order Functions

Shown in Fig. 4 are the results of equivalent electrical input power (EIP) for sin(ω*t) and sin(ω*t)*sin(7ω*t).

3.3 Double modulated Sinusoidal Function

There is a variety of ways higher order sinusoidal functions have upon on the effective equivalent input power (EIP) distribution, as the three graphs in Figure 5 show. They are the results of equivalent input electrical power (EIP) transforms for three different second order, "triply modulated" sinusoidal functions. They are the histograms of EIP delivered by third order, "double modulated" sinusoidal functions: sin(ω*t)*sin(17ω*t)*sin(17 ω*t), sin(ω*t)*sin(13 ω*t)*sin(17 ω*t), sin(ω*t)*sin(17 ω*t)*sin(23 ω*t). The upper curve, [sin(ω*t)*sin(7ω*t)*sin(17 ω*t)], has an EIP distribution shifted toward low powers, with the low-, mid-, and high power regions having 72, 25.8, and 2.2. This heralds a shift toward lower powers, and the acquiring of significant inhomogeneity along the equivalent input power distribution. The bin with the highest density on the histogram analysis was bin 1 with n=60.

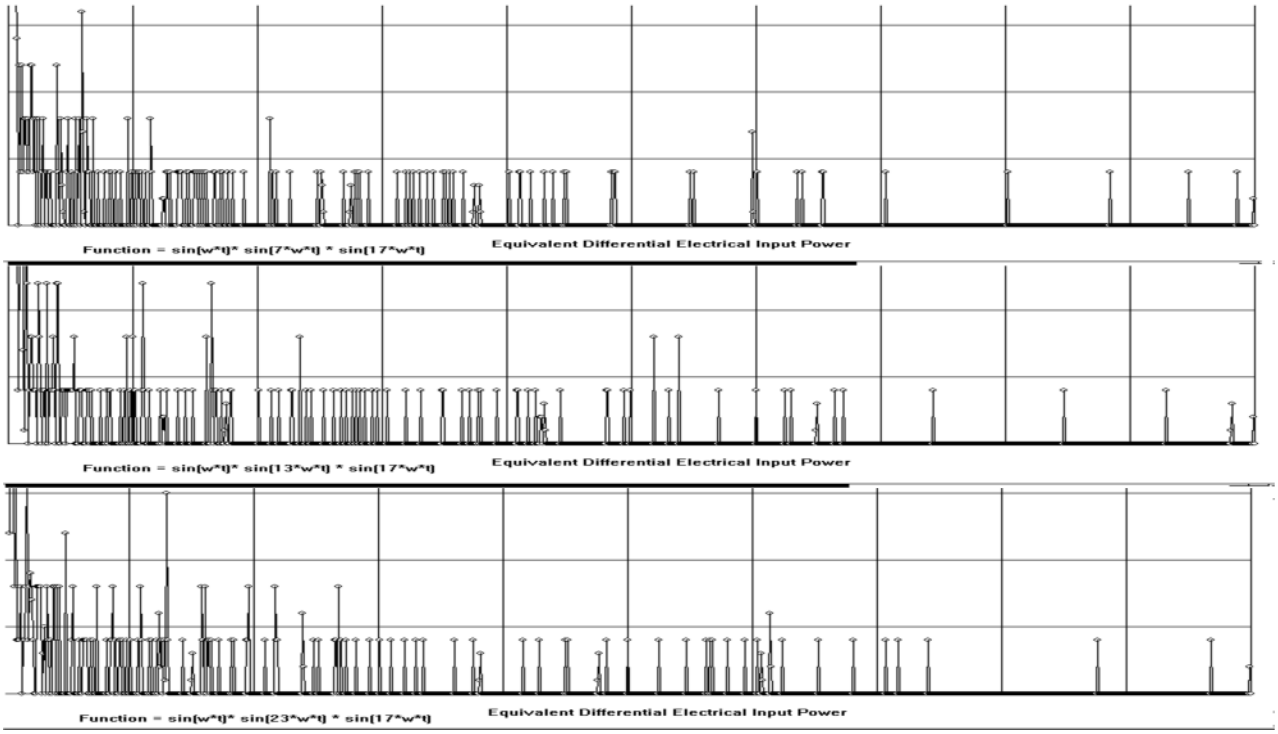

Figure 5. EIP Histograms of 3rd Order Functions

The middle curve, [sin(ω*t)*sin(13 ω*t)*sin(17 ω*t)], is characterized with its EIP sorted into low power, mid power and high power regions as 71.6, 26.2, and 2.2. This heralds a shift toward lower powers, and the acquiring of significant inhomogeneity along the equivalent input power distribution. [The bin with the highest density on the histogram analysis was bin 20 with n=20.]

The lower curve, [sin(ω*)*sin(23 ω*t)*sin(17 ω*t)], was characterized with its EIP sorted into low power, mid power and high power regions as 72.4, 25, and 2.6. This shows a shift toward lower powers, and the acquiring of significant inhomogeneity along the equivalent input power distribution. [The bin with the highest density on the histogram analysis was bin 1 with n=52.]

3.4 The Superwave

Figure 6 shows the histogram of equivalent electrical input power (EIP), the results of this paper's investigation, of the double-modulated "Superwave" function, released and discussed at ICCF-14. The figure shows the EIP histogram for the 'superwave', ie. sin(ω*t)*sin(ω*t)* (1+ ((sin(ω*t)*sin(ω*t))* (1+(sin(ω*t)*sin(ω*t))))). The output covers a wide range of input powers, and there would be a good likelihood of activating a LANR device with this waveform, given its appearance in V*I-space. The disadvantages are low efficiency and that it is not tailored to any specific optimal operating point (OOP) manifold.

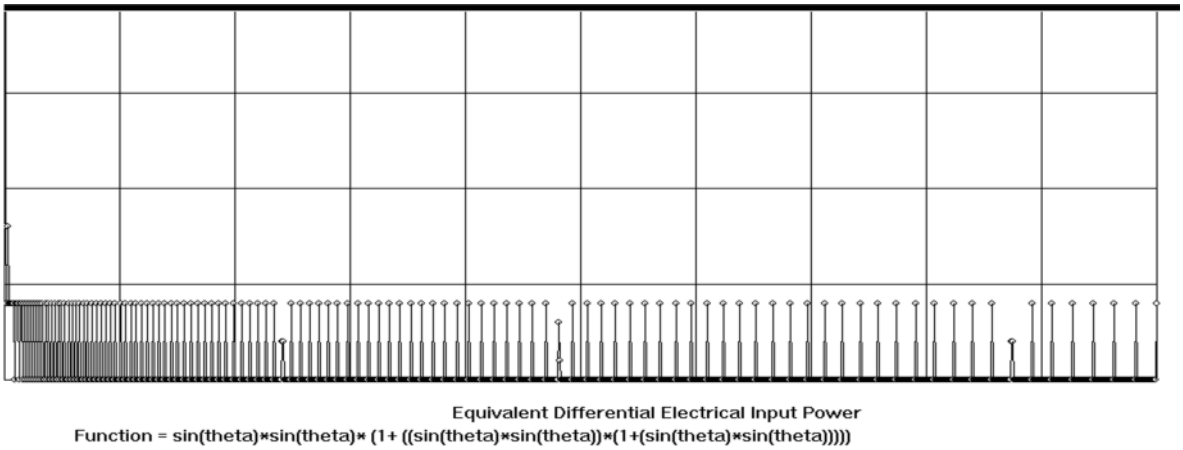

Figure 6. EIP Histogram of Equivalent Electrical Input powers for Superwave

4. Interpretation

This analysis demonstrates that the ´superwave' only functions because it unintentionally drives a LANR system, or device, periodically or intermittently through the OOP peak, thereby giving rise to the desired reaction(s). Although we do not yet know the exact prescription, or precise mathematical wave function of the superwave, the analysis is clear: the superwave, although not as efficient as actually matching the input wave to the optimal operating point of the sample/device, does have some of the input power transferred to the desired reactions.

There are two additional factors that make the hypothesis even more likely. First, this analysis presumes a theoretically 'pure' superwave to calculate the equivalent input power transformation. However, in real life, practical electronics, heat of equipment, and normal operation, yield more complex waveforms, with time-variant electronics, making the "superwave" time variant, affecting the EIP along the input-electrical power axis. Second, actual LANR sample/devices driven by the superwave have a complex behavior, reflect material properties, beyond that modeled here as a simple resistor. Conduction and polarization effects of several types, make for time variant complex behavior (10-12).

As a result of this analysis, it is saliently obvious that the some successful LANR results, such as generated by using the 'superwave' and other driving functions, might actually arise from unintentionally or inadvertently driving the LANR sample, device, or electrode through its optimal operating point at some point during the drive cycle. We refer to those collectively as Hyperdrive™. Also, it is now clear that there is a new important corollary, namely to consider every driving function for its efficiency as pertaining to each of the possible LANR reactions. Some of those may be desirable, and others may not and EIP histograms reveal which specific electrical LANR driving functions are good and useful vehicles and which are not. They also indicate the efficiency of matching the electrical input of an LANR device at its optimal operating point.

5. Conclusions

This study has examined, and has verified as correct, the "Superwave-as-Transitory-OOP-Peak" hypothesis. In this analysis, we have deconvolved the "superwave" (1), and several other similar, and not so similar, LANR driving waveforms, by use of a transformational analysis involving the conversion of a driving time function to its equivalent input power (EIP) manifold. The "Superwave-as-Transitory-OOP-Peak" Hypothesis does offer an explanation of the reported partially successful results of the "Superwave". Based upon the analytical results, including the wave functions and combinations analyzed, such as the EIP histogram results shown in Figures 4 through 6, it is clear that the hypothesis is correct. The "superwave" does, indeed, function, and apparently with less than full efficiency, because it is unintentionally drives the LANR system periodically, or intermittently, through the LANR specimen's OOP peak, and only then giving rise to those desired reactions.

Acknowledgments

The authors thank especially Gayle Verner for her meticulous help, and Pam Boss, Alex Frank, Peter Hagelstein, David Nagel and Scott Chubb for their support and helpful suggestions and JET Energy, Inc. and New Energy Foundation for their additional support. PHUSOR® is a registered trademark of JET Energy, Incorporated. Hyperdrive™ and PHUSOR®-technology are protected by U.S. Patents D596724, D413659 and U.S. Patents pending. © 2010 JET Energy

REFERENCES

1. Dardik, I., H. Branover, A. El-Boher, D. Gazit, E. Golbreich, E. Greenspan, A. Kapusta, B. Khachatorov, V. Krakov, S. Lesin, B. Michailovitch, G. Shani, and T. Zilov, 'Intensification of Low Energy Nuclear Reactions Using Superwave Excitation', Proc. ICCF-10, P.Hagelstein, S. Chubb, World Scientific NJ, ISBN 981-256-564-6, (2006).
2. Dardik, I., Zilov, T., Branover, H., El-Boher, A., Greenspan, E., Khachaturov, B., Krakov, V., Lesin, S., Tsirlin, M. , Progress in Electrolysis Experiments at Energetics Technologies (PowerPoint slides). in The 12th International Conference on Condensed Matter Nuclear Science. 2005. Yokohama, Japan.
3. Dardik, I., et al.,14th International Conf. on Condensed Matter Nuclear Science (2008).
4. Swartz, M, "Consistency of the Biphasic Nature of Excess Enthalpy in Solid State Anomalous Phenomena with the Quasi-1-Dimensional Model of Isotope Loading into a Material", Fusion Technology, 31, 63-74 (1997).
5. Swartz, M, "Optimal Operating Point Characteristics of Nickel Light Water Experiments", Proceedings of ICCF-7 (1998)
6. Swartz. M., "Generality of Optimal Operating Point Behavior in Low Energy Nuclear Systems", Journal of New Energy, 4, 2, 218-228 (1999).
7. Swartz. M., "Control of Low Energy Nuclear Systems through Loading and Optimal Operating Points", ANS/ 2000 International Winter Meeting, Nov. 12-17, 2000, Washington, D.C. (2000).

8. Swartz. M., G. Verner, "Excess Heat from Low Electrical Conductivity Heavy Water Spiral-Wound Pd/D_2O/Pt and Pd/D_2O-$PdCl_2$/Pt Devices", Condensed Matter Nuclear Science, Proceedings of ICCF-10, Pages 29-44 (2006).
9. Swartz. M., G. Verner, "Can a Pd/D_2O/Pt Device be Made Portable to Demonstrate the Optimal Operating Point", ICCF-10 (Camb. MA), Proceedings of ICCF-10, (2003), Condensed Matter Nuclear Science, Proceedings of ICCF-10, pages 45-54, (2006).
10. A. von Hippel, ed., "Dielectric Materials and Applications", MIT Press (1954).
11. A. von Hippel, D.B. Knoll, W.B. Westphal, "Transfer of Protons through 'Pure' Ice I_h Single Crystals", J. Chem. Phys., 54, 134, (also 145), (1971).
12. Swartz, M., "Quasi-One-Dimensional Model of Electrochemical Loading of Isotopic Fuel into a Metal", Fusion Technology, 22, 2, 296-300 (1992).